THE DEVELOPMENT AND TESTING OF A NOVEL AUTOMATIC ORGANOID/MICROSPHERE MOVEMENT DEVICE

A Technical Report submitted to the Department of Biomedical Engineering

Presented to the Faculty of the School of Engineering and Applied Science

University of Virginia • Charlottesville, Virginia

In Partial Fulfillment of the Requirements for the Degree

Bachelor of Science, School of Engineering

Kaden Hoffman

Spring, 2023

Technical Project Team Members

Remington Martinez

Jack Maschler

Josh Sanderson

On my honor as a University Student, I have neither given nor received unauthorized aid on this assignment as defined by the Honor Guidelines for Thesis-Related Assignments

Chris Highley, Department of Biomedical Engineering

The Development and Testing of a Novel Automatic Organoid/Microsphere Movement Device

Abstract

Organoid research has exploded in the past decade going from 84 publications to over 3000 in 2022. With exponential growth like that streamlining the process of setting up organoid studies becomes increasingly important. Here we present a proof-of-concept study of our novel device that automatically withdraws and deposits hydrogel microparticles in user-defined locations. This device uses commercially available products and CAD-created components paired in a Python-programmed embedded system to identify microparticles within a 96-well plate, pick them up, and place them into a specified location in a 12-well plate. In a 50-sample movement trial, the cumulative success rate of the device was 45.97% or 23 out of 50 particles successfully detected, withdrawn, and deposited in the desired location. When the speed of moving 10 particles was compared to the manual alternative, the device was initially slower before the fourth particle but then surpassed the human subject likely due to fatigue. Over the movement of 10 microparticles, the device was significantly faster than the manual alternative ($p = 0.0094$). These results suggest that our device is a viable option and a swifter alternative to the current standard for moving organoids/microparticles: manual vacuum aspiration. If further iteration of the pick-up and placement modality increases the cumulative success rate, it is likely that this device would dramatically increase the scalability and scope of organoid studies by decreasing active and training time necessary to move organoids and improving the accuracy and precision of organoid placement.

Keywords: Organoid, Spheroid, Automatic Movement

Introduction

Overview

Organoids are three-dimensional cell cultures constructed from stem cells that function to mimic human organs in-vitro. Human stem cells were first successfully harvested in 1998, however, the first true organoid was not developed until 2009 when Sato et al. derived the first organoid from a single adult stem cell (ASC) seeded in Matrigel, a hydrogel material[1]. The landmark study in 2009 demonstrated that the key factor in the induction of ASC differentiation, and thus organoid formation was the biomaterial and environment in which it was seeded[1]. Since then, many different organoids have been developed and used to study diseases, develop drugs, and even the preliminary development of transplantable organs[2]. Although the range of organ tissues that can be mimicked in-vitro using organoids has increased dramatically, their use in research remains limited by their lack of freedom of mobility [3].

ASCs are placed into biomaterials by hand using a pipette and once differentiated into organoids, moved to imprecise locations via vacuum aspiration[4]. Although effective for small-scale studies where precision is less of a critical variable, the current organoid movement method is time-consuming, imprecise, and limits the scale and scope of potential studies[3]. As with any procedure that relies heavily on human manual dexterity, the placement of organoids into specific locations within biomaterials is imprecise, thus introducing error and limiting study conclusions[3]. Vacuum aspiration itself also introduces error through the accompaniment of media with organoid deposition. The extra media deposited with the organoid alters the desired extracellular environment, again limiting conclusions that can be made[5]. By improving the current movement method of stem cells and organoids, new research could be conducted with higher degrees of accuracy and a faster turnaround time. Additionally, a more precise placement method would open the possibility for more abstract organoid arrangements to better mimic in-vivo conditions[6].

Here, we aim to design and construct a device that precisely places organoids into a designated position in a

permissive biomaterial using an automated set-it and forget-it approach. As aforementioned, there is currently no automatic way to withdraw and deposit organoids, thus this paper presents a novel device that may potentially remedy that shortcoming. Given the novel nature of our device and the two-semester timeline, the scope of this study is limited to that of a proof-of-concept to show that our device (1) successfully withdraws and deposits hydrogel beads and (2) does so faster than if it was done manually.

More specifically, we have designated two aims for our project which have been accomplished. **Aim 1** consisted of designing and constructing a device with multiaxial movement capabilities that can hold all the necessary components for image detection and organoid movement using existing or CAD-created components. In order to accomplish Aim 1 we utilized Fusion 360 and laser printing technology to develop 3D components capable of holding well plates, a high-resolution camera, and a nano-injector (Figure 1). Second, we integrated linear guide rails and NEMA-23 motors that are capable of moving the components on all three axes. In conjunction, these components allowed for automated movement of the well plates, the camera, and the nanoinjector, which is necessary for organoid withdrawal and deposition. To integrate the aforementioned components **Aim 2** sought to develop a Python program to automate the system in which organoids are moved into a biomaterial. This was achieved by creating a unified communications network between all components and designing a system that requires minimal human input in order to remove human error and reduce the operational hours of manual labor.

By accomplishing the aforementioned aims and subjecting the device to proof-of-concept trials, we show that our novel device has the potential to be both more efficient and effective than the current manual alternative. Thus, future iterations of our device will save countless hours for researchers while also increasing the reliability and scalability of their organoid-reliant studies.

Materials and Methods

Multiaxial movement and device holding capabilities

The base of the device is derived from a prebuilt multi-axial sled movement system containing a system of linear guide rails as depicted in Figure 1. The movement in the device is powered by NEMA 23 motors that are controlled by a Python system and connected to a GUI. A 12V AC to DC converter is used to power these motors. Three of these motors are used, one on each axis, to allow for the multiaxial movement necessary for this device to serve its purpose. The two motors on the horizontal axes motors are used to move both a 96-well plate containing the organoid(s) and a plate containing the permissive biomaterial into which the organoids will be seeded, which are both held in a purchased holding device as shown in Figure 1. The motor on the vertical axis of the device allows for the vertical movement of the Basler Ace camera and 2020 Nanoliter injector to allow for both the image detection of organoids by the camera and the withdrawal and deposition of organoids by the injector. Both the

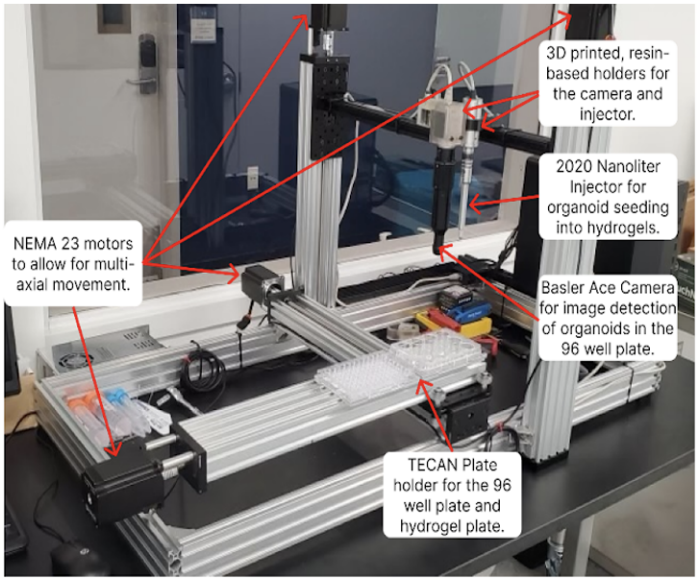

Figure 1: Hardware components of an automated organoid seeding device.

camera and injector are held in place on one of the linear guide rails using 3D-printed holders that allow for minimal shaking in these devices. These components required a few rounds of iteration in order to fit the needs of this device. For the camera holder, the initial design placed the camera too close to the well plates, resulting in contact and inaccurate image detection. To remedy this, a buffer component was created to increase the height at which the camera sat in the device, allowing for more accurate image detection. For the injector component, the initial design was built to allow the attachment component of the injector to sit in the holder and then be screwed into the

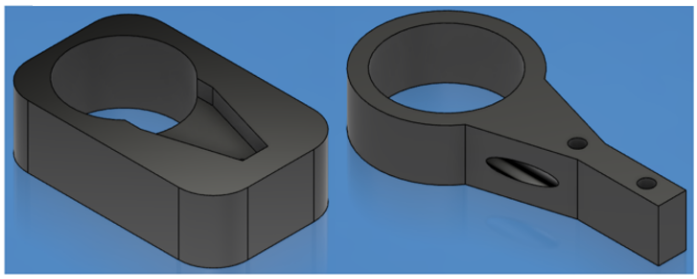

Figure 2: Comparison of initial and final design of 3D CAD design of 2020 Nanoliter injector holder.

guide rails. While effective in holding the injector, this design required all of the holding force to be put on one end of the design, ultimately leading to the deformation of the device upon repeated use. This deformation caused crooked and imprecise movement of the injector. To remedy this issue, we altered the design so that the attachment component of the injector was actually removed and instead built into the holder, the design change can be seen in Figure 2. This allowed us to not only screw the holder into the guide rails but also directly into the injector, leading to a better dispersion of holding force and thus less deformation in the holder. The final configuration of these devices in the system can be seen in Figure 1. For the image detection done by the camera to be accurate, there must be uniform lighting of the target, and as such, the device must be used in an area containing uniform lighting[7].

Python-Controlled Automation of the entire Device

Embedded systems are specially designed computer systems meant to function as a part of a larger machine with the purpose of controlling services to the system. The Universal Serial Bus (USB) standard has been implemented to allow for serial communication across the computer's serial ports to allow for ease of debugging between the stepper motors, camera, and injector. This USB standard functions by creating a logical connection between the host and device endpoints in a method known as piping which transfers data bytes known as packets across the USB communication system. Token packets allow for OUT or IN token references in which the data is either written to or read from the device with expected data packets being sent or received, respectively[8]. Through this, data from the camera can be read while bit transfers are sent to the stepper motor and injector to move the device within the triaxial system and allow for more precise microsphere/organoid pickup. Once the user has inputted an organoid formation into the GUI and placed a 96-well plate of organoids into the plate holder, the camera will begin image detection of the 96-well plate. Using the Python system, the camera will systematically determine if an organoid is present in each well. When new cells are created, the machine inherently does not know where they are. As such, images are saved to a training diagram in which an 80%, 20%, and 10% split is created (Figure 3). Permutations are made around the user's inserted data to allow for the correlation between new positions, differing saturation and brightness levels, and with repositioning to generate synthetic data. This allows for a higher training amount as compared to the standard method of hand labeling although it may not show as good of recall (reference the original fluorophore data that was made by hand over 300 images with the new hydrogel synthetic 300 image amount).

After completing this process, the organoid's location in each well will be communicated to the motors and Nanoliter injector through the Python communication network as described previously. The motors will then move the Nanoliter injector to the location of the first organoid to be seeded, which will be the bottom leftmost well. The injector will then be moved down into the well where the suction system of the injector will be activated to capture the organoid. Next, the motors will move the injector up and over to the designated location in the permissive biomaterial, where the injector will again be lowered to the desired depth in the biomaterial. The injector will then be told by the Python system to release the organoid. This process will be repeated until all of the user-selected formations have been completed. The entirety of this process will be completely controlled by the Python communication network and thus fully automated outside of the user selecting their desired organoid formation[9].

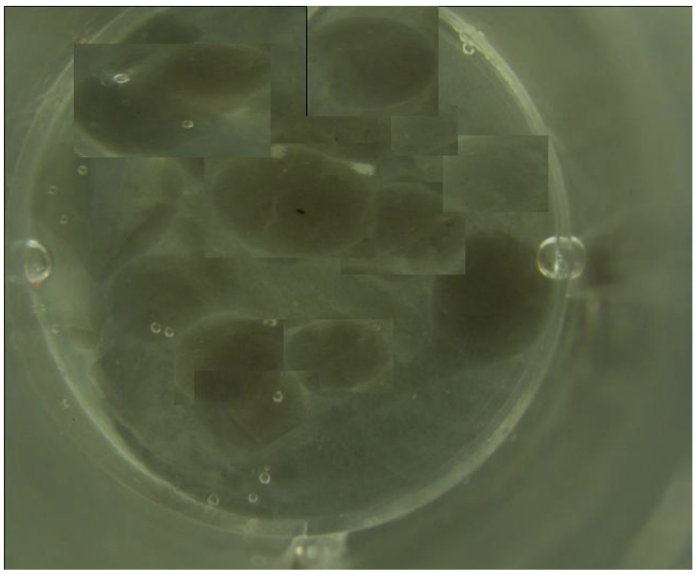

Figure 3: Illustration of the microparticles being imaged for image detection using a machine learning algorithm.

Testing Methods

The calibration of the image detection software was determined by having the program predict the coordinates of the bounding box around the spheroid when a spheroid is present in the image, as seen in Figure 4, where the algorithm has created a bounding box around a fluorophore. The coordinates of ground truth and predicted bounding boxes are then compared and the mean-square

error is calculated. The actual precision of the image detection software was measured as the percentage of predictions from the previous data that are correct as a

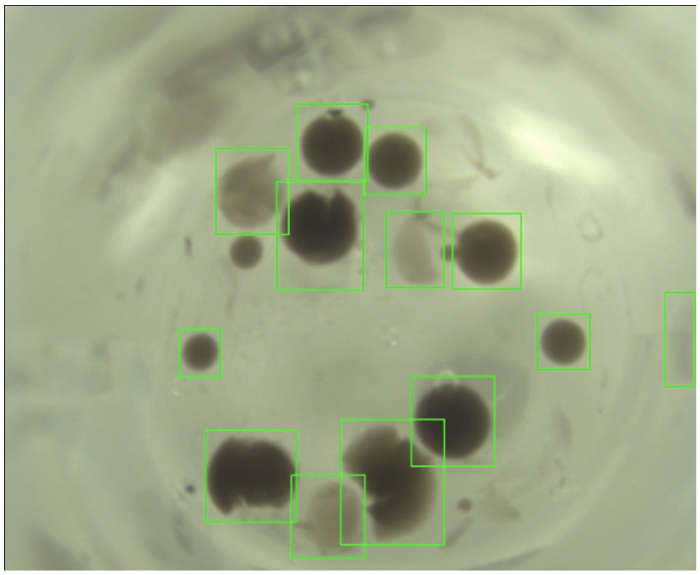

Figure 4: Image of a single well containing microparticles that have gone through image detection and have been traced by the software.

measure of True Positive (TP)/ (TP + False Positive). To test the image detection and pickup/placement capabilities of this device, microparticles and fluorophores were suspended separately into an aqueous solution and randomly dispersed into wells of a 96-well plate[10]. For our initial testing, we treated hydrophobic fluorophores using a tween-based method involving the boiling of deionized water and the use of an immersion blender as described by Cospheric LLC[11]. This method effectively "coats" the hydrophobic fluorophores so that are able to interact with a hydrophilic environment, in this case, water. This method did not end up showing promising results as elaborated upon in the discussion section, thus, hydrophilic hydrogel beads were constructed for the remainder of the testing. Once the algorithm is trained using the aforementioned method, the image detection portion then detects and traces what it believes to be particles in the well. An image of the traced particles is presented and then we recorded how many particles were actually in the well, how many the program recognized, and how many false positives the program produced. Next, the program chooses a particle and begins to pick the particle and transfer it to the 12-well plate where it places the particle. For this portion, we recorded whether or not the injector hit the targeted particle or fluorophore, whether it displaced the particle or fluorophore, whether it picked up the particle or fluorophore, and whether the injector successfully placed the particle or fluorophore. This was repeated for a total of 50 trials for both the microparticles and fluorophores. In comparison to seeding done by hand, the effectiveness of this device in terms of speed was tested by having a trained, unbiased individual pick up and place 10 microparticles consecutively[12]. The same process was completed by our device. Additionally, these trials were timed and the split for each individual particle was recorded to determine the effect of fatigue on the manual trials.

Results

Design Constraints

It is possible that the motors used for the multiaxial movement do not receive the full 12V from the power source, which may lead to inaccurate movement of the devices by the motor. This is accounted for by testing the voltage across the motor using a multimeter so this is unlikely to affect the performance of the device[13]. The 12V power source is also a constraint as this power cap limits the speed at which the components can be moved and thus the speed at which the device can work. However, we believe that the speed at which the motors can move the guide rails with a 12V power source (0.023 mm/s) is sufficient to meet the aims and goals of this project. An additional design constraint is that the horizontal linear rail is slightly elevated which causes the injector to touch the bottom of the well too closely. This could result in the organoid not being released properly; however, we have not seen any limitations to this with the microparticles. Correspondingly, the depth from the camera to the bottom of the well was measured by hand, which limits our precision of the distance needed to lower the injector in order to pick up a particle.

The step size of the NEMA 23 stepper motors could limit the accuracy of organoid seeding as this determines the minimum distance the injector can move at a time. However, we have not seen this significantly affect the performance of the device as the step size in this device is 14 microns, which is small enough to place organoids within the 100 micron threshold for success. There is also the possibility of misclassification within the dataset where the user erroneously classifies an image which could degrade the accuracy of the training model or have an organoid that can not be trained through the neural network using the priori model and would require a data-dependent method and stringent testing to view the model classification to ensure limited false discoveries within the dataset[14].

A potential constraint of the image detection capabilities of the device is that despite efforts to create uniform lighting around the plates, there are still variations in light levels. This could lead to inaccuracies in detecting the presence of organoids, which would limit the ability of the device to seed said organoids into the biomaterial[7]. A constraint involving the ability of the device to pick up and move the organoids is that since organoids vary in size, the capillary tube of the Nanoliter injector may not be able to pick up all types of organoids. The capillary tube has a diameter of 1.5 mm, meaning that organoids with significantly larger diameters will likely be unable to be picked up by the device. However, organoids are typically 0.4-0.7 mm in diameter, so this is not likely to be an issue[15] Additionally, the processing power of the hardware is a further constraint as not having enough computational power could lead to prolonged periods of computer calculations and an inability for the device to perform under 60 minutes. Ideally, the device and hardware required to run the software would be low with regards to the computational power, having an idealized minimum requirement of a Raspberry Pi, which would allow for large-scale deployment and more potential refinement of the final device design. Having limited processing power directly affects the system's ability to run the convolutional neural network on training data, create prediction sets, and implement serial bus commands to interact with the attached devices to move the spheroids. An i7-7500U can train, on average, 115 samples per second, while a Raspberry Pi can expect to take around three samples per second[16]. As such, our current device will have the limitations of requiring a minimum CPU boost speed comparable to an i7-6850k@3.60 GHz with 16 GB of memory to allow for rapid computation of the neural network[17].

Device Testing Iterations

As mentioned in the materials/methods section, our first test involved attempting to move fluorophore particles between the 96-well and 12-well plates. Fluorophore particles were originally chosen for ease of sight and cost-effectiveness, however, the withdrawal and deposition rates were poor due to the particles having a tendency to stick to the glass of the capillary connected to the nano-injector. Out of 50 trials, only one trial was considered successful, that is, the fluorophore was correctly detected, picked up, and placed in the 12-well plate (Figure 5).

Given the unfruitful nature of the testing with the fluorophores, we retrained the algorithm to detect black-dyed hydrogel beads, a nonliving particle of similar diameter and hydrophilicity to organoids and cell spheroids[18]. In the preliminary testing with these particles, particle displacement occurred as the nano-injector broke the surface of the water in the 96-well plate. This caused the nano-injector to fail in picking up the particle the algorithm had detected as it had moved after the completion of the image detection. To circumvent this issue, we implemented a delay right after the nano-injector broke the surface of the water which dramatically decreased the frequency of the particle displacement. After being able to successfully pick up and place the hydrogel beads more reliably, we conducted 50 trials to assess the algorithm's image detection success rate, the number of false positives per trial, whether the injector moved properly to the algorithm detected location (hit), and

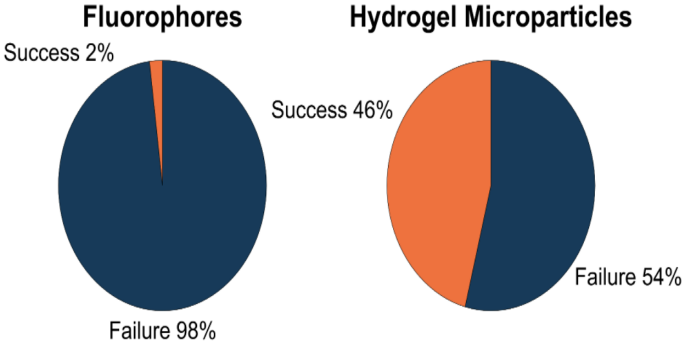

Figure 5: Pie chart displaying the success rate of pick up and placement of fluorophores and hydrogel microparticles by the device.

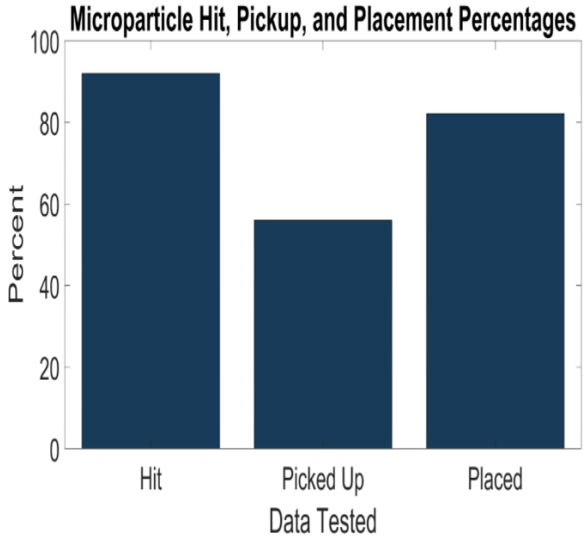

Figure 6: Bar graph displaying the hit, pickup, and place percentages of the device when testing with microparticles.

finally the withdrawal and deposition rate. The algorithm successfully identified 100% of the particles in 42 out of the 50 trials and had a cumulative success rate of 96.33% (367 detected out of 381 present). With respect to false positives, defined as a particle detected that is not actually a particle, the average was 0.7 ± 0.76 beads (average ± standard deviation) per trial. As illustrated in Figure 6 the particles were successfully picked up 56.0% of the time and successfully placed 82.1% of the time. Together this gives a cumulative success rate of 45.97% which indicates that out of the 50 trials, 23 out of 50 particles were successfully detected, withdrawn from the 96-well plate, and deposited into the 12-well plate (Supplementary Video 1).

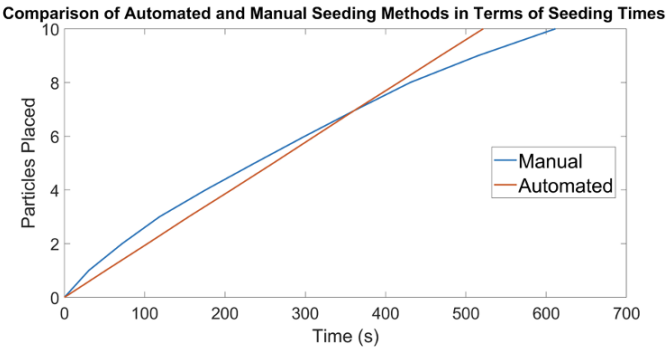

Figure 7: Line graph comparing the seeding times between automated and manual methods.

In addition to testing the effectiveness of the device, we tested its efficiency as compared to the manual alternative. As shown in Figure 7 the device maintained a relatively constant withdrawal and deposition rate while the subject took more time with each additional particle withdrawn and deposited. Although the subject was initially quicker at moving the particles, by the fourth particle moved the device had already caught and surpassed the subject. Over the movement of just 10 particles, the device took statistically significantly less time to pick up and place the microparticles in comparison to the manual method. The difference between the time splits for the automated and manual methods was determined using a Student's T-test, which resulted in a p-value of 0.0094, indicating statistical significance.

Discussion

Interpretation of Testing

Fluorophore Test

As discussed in the previous section, the movement testing with the fluorophore particles did not produce ideal results. However, the results suggest that despite being treated with tween-20 to become hydrophilic, the inherent hydrophobic nature of the particles remains prominent in their behavior in water. Additionally, this test highlighted a key aspect of our device that is important to note. Given the hydrophobic nature of glass and our use of capillaries in our movement method, it is likely that strongly hydrophobic particles will have a lower success rate due to the nano-injector supplying insufficient force to break the adhesion between the hydrophobic particle and the glass capillary.

Hydrogel Bead Test

Although the cumulative success rate of the device was only 45.97%, the relatively high identification rate of 96.33%, and the 0.7 average false positives per trial suggest that neither the camera, the motors/track, nor the algorithm is the main source of the lower-than-ideal cumulative success rate. This leaves the nano-injector as the final variable that might be limiting the success rate. This is in line with our expectations as the nano-injector is not specifically designed for this application and has a limited volume that can assist in the withdrawal and deposition of the particles. Despite the low success rate, the results still show that our device can indeed accomplish the task of moving hydrogel microparticles with a set-it-and-forget-it approach.

Machine versus Man

As mentioned in the results section, the device could withdraw and deposit hydrogel microparticles significantly faster than the subject after only the seventh bead moved ($p=0.0094$). This is in line with our expectations as humans are susceptible to distractions, fatigue, and boredom when it comes to monotonous tasks like picking up and placing hydrogel beads. Given that such a robust difference was present in a small-scale trial of only 10 beads, it is reasonable to assume the result would be drastically more profound in a trial that is an order of magnitude larger. Thus, these results suggest that our device is an effective alternative to the manual method with respect to speed, especially for sample sizes larger than four beads.

Limitations

Although the results of our testing show the proof-of-concept that our device can withdraw and deposit hydrogel beads and do so faster than the manual alternative, there are still some limitations with respect to the scope of our testing and results. First, the amount of time provided to construct and test the device was limited to two semesters with all team members having other

additional scholarly obligations. This decreased the amount of time available to iterate on the design and potentially ideate a better movement modality than the nano-injector. Second, in order to both save time and mitigate costs, all testing was done with non-living particles rather than organoids themselves. This limits the conclusions that can be drawn from our results as it is possible that the hydrogel microparticles interact with the movement system differently than living organoids or cell spheroids. Finally, the aforementioned time constraint decreased the number of trials where we could test both the effectiveness of the device and the speed compared to a human subject.

Impact

Despite the limitations to our testing and the device itself, our results are promising as preliminary efforts to increase the scalability of organoid and cell spheroid studies while also decreasing the amount of active and training time required to conduct them. With continued iterations of our design and further testing, it is likely that the cumulative success rate can dramatically increase, making it a viable option for research labs across the globe.

Future Work

By continuing to iterate on the design while consistently testing with hydrogel microparticles we believe that we can achieve a higher cumulative success rate. Additionally, we believe iteration efforts should be focused on either improving the ability of the nano-injector to withdraw and deposit the beads or developing a new pickup and placement method altogether as that was likely the source of the low success rate in the trials above. After achieving a success rate of 85%, testing with organoids and cell spheroids should be conducted to see if the success rate stands despite using living cells. It is likely that the success rate will stand given the similar external properties between the hydrogel beads and the organoids, but if it does not, further iteration should involve switching the 96-well plate from a flat bottom to a curved bottom and adding an additional camera so that the algorithm can detect the organoid's position in three dimensions rather than just two. Once the organoid tests are successful, the device can move from the prototype phase to the design for the manufacturing (DFM) phase while a patent for the movement method is filed. During the DFM phase, the device aesthetic and size footprint should be significantly streamlined so that there is no erroneous material and that it can fit in a traditional lab space. Additionally, software developers can be brought on to improve the user experience with the GUI and to add more placement options for the user to input into the GUI. Finally, after these iterations have been made, the device will be ready for the market.

End Matter

Author Contributions and Notes

Hoffman, K., Maschler, J., Martinez, R., and Sanderson, J., created CAD designs, constructed prototypes, developed the algorithm, designed and conducted trials, and wrote the final report. Highley, C. created the hydrogel beads, supplied funding, and advised when issues arose. The authors declare no conflict of interest.

Acknowledgments

The capstone team would like to thank Dr. Christopher Higley from the UVA Department of Biomedical Engineering for advising the research and development of the device. The team would also like to thank Dr. Timothy Allen and Dr. Shannon Barker from the capstone teaching staff in the UVA Department of Biomedical Engineering for advising throughout the project.

Supplementary Video:

a) Supplementary Video 1
https://youtu.be/v_N2w09sM6E

References

1. Sato, T. *et al.* Single Lgr5 stem cells build crypt-villus structures in vitro without a mesenchymal niche. *Nature* **459**, 262–265 (2009).
2. Magno, V., Meinhardt, A. & Werner, C. Polymer Hydrogels to Guide Organotypic and Organoid Cultures. *Adv. Funct. Mater.* **30**, 2000097 (2020).
3. Ren, Y. *et al.* Developments and Opportunities for 3D Bioprinted Organoids. *Int. J. Bioprinting* **7**, 364 (2021).
4. Daly, A. C., Davidson, M. D. & Burdick, J. A. 3D bioprinting of high cell-density heterogeneous tissue models through spheroid fusion within self-healing hydrogels. *Nat. Commun.* **12**, 753 (2021).
5. Protocol for Application, Standardization and Validation of the Forskolin-Induced Swelling Assay in Cystic Fibrosis Human Colon Organoids: STAR Protocols. https://star-protocols.cell.com/protocols/72.
6. Yin, X. *et al.* Stem Cell Organoid Engineering. *Cell Stem Cell* **18**, 25–38 (2016).
7. Makihara, Y., Takizawa, M., Shirai, Y. & Shimada, N. Object Recognition under Various Lighting Conditions. in *Image Analysis* (eds. Bigun, J. & Gustavsson, T.) vol. 2749 899–906 (Springer Berlin Heidelberg, 2003).
8. Debugging Serial Buses in Embedded System Designs | Tektronix. https://www.tek.com/en/documents/application-note/debugging-serial-buses-embedded-system-designs-0.
9. Banerjee, D. *et al.* Strategies for 3D bioprinting of spheroids: A comprehensive review. *Biomaterials* **291**, 121881 (2022).
10. Image Recognition and Classification in Python with TensorFlow and Keras. *Stack Abuse* https://stackabuse.com/image-recognition-in-python-with-tensorflow-and-keras/ (2019).
11. Tween solutions for Suspension of Hydrophobic Particles in Water for Density Marker Beads in Percoll or other gradients or Flow Visualization. https://www.cospheric.com/tween_solutions_density_marker_beads.htm.
12. Zihni, A. *et al.* Comparison of precision and speed in laparoscopic and robot-assisted surgical task performance. *J. Surg. Res.* **223**, 29–33 (2018).
13. ANIZIOL. How To Check If an Electric Motor Is Going Bad. *Moley Magnetics* https://www.moleymagneticsinc.com/how-to-check-if-an-electric-motor-is-going-bad/ (2020).
14. Xu, Y. & Goodacre, R. On Splitting Training and Validation Set: A Comparative Study of Cross-Validation, Bootstrap and Systematic Sampling for Estimating the Generalization Performance of Supervised Learning. *J. Anal. Test.* **2**, 249–262 (2018).
15. Singh, S. K. *et al.* Critical role of three-dimensional tumorsphere size on experimental outcome. *BioTechniques* **69**, 333–338 (2020).
16. Glezer, M. Running a Convolutional Neural Network on Raspberry PI. *The Startup* https://medium.com/swlh/running-a-convolutional-neural-network-on-raspberry-pi-4fc5bd80aa4d (2020).
17. Table 1 . Hardware specifications to learn the CNN. *ResearchGate* https://www.researchgate.net/figure/Hardware-specifications-to-learn-the-CNN_tbl2_323782871.
18. Core-shell hydrogel beads with extracellular matrix for tumor spheroid formation - PMC. https://www.ncbi.nlm.nih.gov/pmc/articles/PMC4401801/.